Electropolymerization of Pyrrole and Electrochemical Study of Polypyrrole. 5. Controlled Electrochemical Synthesis and Solid-State Transition of Well-Defined Polypyrrole Variants

Ming Zhou,[†] Markus Pagels, Beate Geschke, and Jürgen Heinze*

Institute for Physical Chemistry, Albertstrasse 21, Freiburg Materials Research Center, Stefan-Meier-Strasse 21, Albert-Ludwigs-University of Freiburg, D-79104 Freiburg, Germany

Received: April 29, 2002; In Final Form: July 12, 2002

Under well-controlled conditions, different polypyrrole variants can be galvanostatically prepared in acetonitrile + 1% H_2O by changing the current density. At current densities down to 0.25 mA/cm^2, PPy(I) is electrosynthesized; at lower current densities, a mixture of PPy(I) and PPy(II) is generated. In the presence of a small amount of acid ($\sim 1 \times 10^{-5}$ M), PPy(II) is exclusively formed. The availability of well-defined materials enables us to perform further reliable characterization by EQCM. The results reveale different natures of ionic transport when different PPy variants are switched between oxidized and neutral states. When doped with PF_6^-, PPy(I) and PPy(III) show only anionic movement upon redox, whereas PPy(II) exhibits the transport of both anion and cation. The structural diversity of PPy explains some controversial results that were obtained in the past. The mechanistic analysis offers new insight into the formation paths of conducting polymers. Of particular interest is the electrochemical solid-state transition from PPy(II) to PPy(I) in pyrrole-free solution when a higher potential (>1.4 V) is applied to the PPy(II)-coated electrode. Repetitive potential scans transform PPy(II) completely into PPy(I). The transition is clearly evidenced by voltammograms. EQCM demonstrated a consistent change in ionic movement. In situ conductivity measurements indicate different types of charge carriers generated during the charging of PPy(I) and PPy(II).

Introduction

Electrochemical oxidation of heterocycles such as pyrrole,[1] thiophene,[2] and their derivatives induces a cascade of chemical and electrochemical reactions, which eventually produce conducting polymer films on the electrode. Because of the similarities between the first step (formation of radical cations[3,4]) and the last step (formation of resulting polymers), the specific chemistry of individual monomers has been more or less neglected in generally accepted reaction schemes. On the basis of a systematic voltammetric investigation of the electropolymerization of pyrrole, we observed unambiguously the diversity[5,6] of polypyrrole (PPy) and, accordingly, proposed a mechanism[6] involving multipathways to PPy variants. According to these findings and suggestions, the electrosynthesized PPy is generally composed of several variants. Optimized and well-defined PPy can be prepared under controlled conditions. In the case of PF_6^- -doped PPy, two variants showing well-shaped voltammograms can be clearly distinguished. PPy(I), which is the dominant component of PPy normally prepared under mild conditions, has an oxidation wave at ca. 0.0 V (vs Ag/AgCl; the same reference is employed hereafter in this paper) and a reduction wave as high as the oxidation wave at a potential of −0.28 V. PPy(II), which is generated at very low formation potentials or reaction rates in weakly acidic acetonitrile, has a sharper oxidation wave at ca. −0.23 V and a fairly broad, much weaker reduction wave at −0.37 V. PPy(III) is a partially conjugated copolymer with both saturated pyrrolidine and unsaturated pyrrole rings in a polymeric network. The acid-catalyzed trimerization[7] of pyrrole and the follow-up electrochemical and chemical reactions[6,8] play a crucial role in the formation of PPy(III). These results provide new insights into the properties of PPy and the electrochemistry of pyrrole. Nevertheless, the properties of these PPy variants have been characterized only voltammetrically, and many questions concerning the structures and properties of the well-defined PPy variants remain open. One certainty is that the chain-propagation mechanism for the growth of conducting polymers as proposed by Diaz[1d] can be excluded. In that case, only the rate of polymerization should decrease, depending on the applied formation potential. However, all data clearly show that the structure of the resulting polymer is a function of the highest electrode potential applied during the electrochemical polymerization. In this paper, we present new results concerning the generation of structurally different types of polypyrrole. We report the galvanostatical electrosynthesis of the well-defined PPy(I) and PPy(II) and their characterization by EQCM (electrochemical quartz crystal microbalance) and in situ conductivity measurements. In addition, we will describe the electrochemical solid-state transition from PPy(II) to PPy(I).

Experimental Section

Chemicals. Pyrrole (Aldrich) was distilled under argon from CaH_2 immediately before use. Acetonitrile (Fisons, HPLC solvent) and deionized water were purged with argon for half an hour before use. The basic active alumina powder (ICN alumina B-Super I) and supporting electrolyte tetrabutylammonium hexafluorophosphate ($TBAPF_6$, Fluka, electrochemical grade) were dried as described below.

Alumina was loaded into the column of the electrochemical cell and vacuum-dried at 300 °C for 2.5 h. After the cell cooled to room temperature, $TBAPF_6$ was added to the cell, followed by evacuation of the cell at room temperature for half an hour.

* Corresponding author. E-mail: juergen.heinze@physchem.uni-freiburg.de.
[†] Present address: Building M-50, Institute for National Measurement Standards, National Research Council of Canada, 1200 Montreal Road, Ottawa, Ontario, K1A 0R6, Canada.

10.1021/jp0210778 CCC: $22.00
Published on Web 09/11/2002

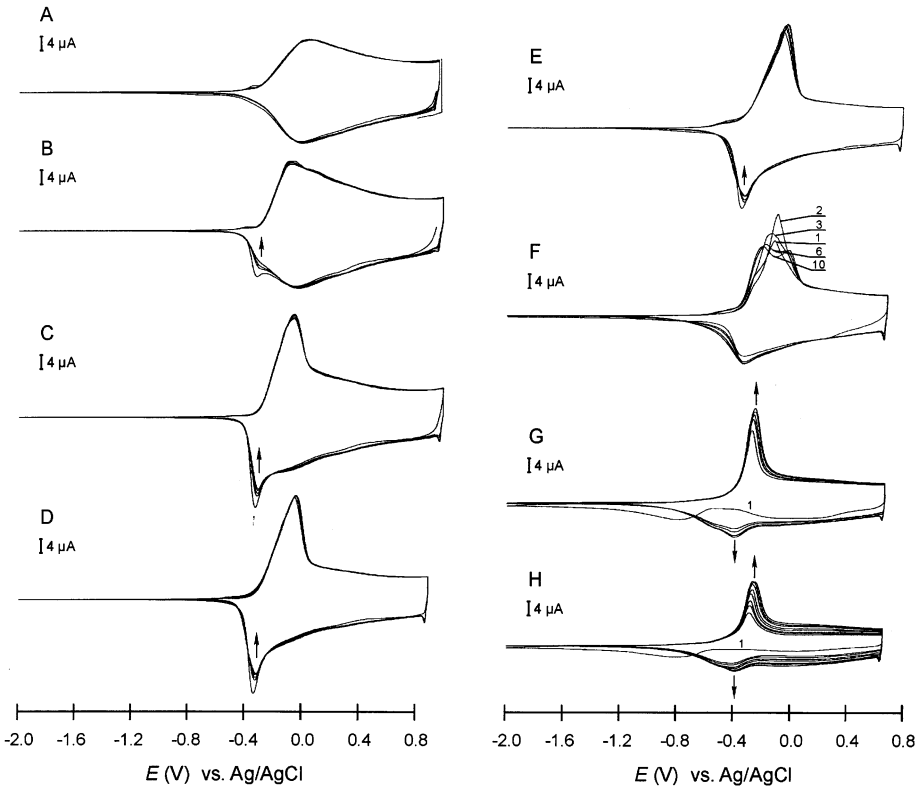

Figure 1. CVs of PPy variants galvanostatically prepared at different current densities. Monomer-free solution: 0.1 M $TBAPF_6$ in acetonitrile, 100 mV s^{-1}, 20 °C. Preparation solution: 0.1 M pyrrole, 0.1 M $TBAPF_6$, 1 wt % H_2O, 1% 10^{-5} M HCl in acetonitrile, 20 °C. (A) 200 μA/1.007 mC, 1.01 to −1.99 V; (B) 150 μA/1.072 mC, 1.01 to −1.99 V; (C) 100 μA/934.8 μC, 1.01 to −1.99 V; (D) 50 μA/783.2 μC, 0.91 to −1.99 V; (E) 2 μA/721.5 μC, 0.81 to −1.99 V; (F) 0.5 μA/720 μC, 0.71 to −1.99 V; (G) 100 nA/720 μC, 0.69 to −1.99 V; (H) 50 nA/720 μC, 0.68 to −1.99 V. (Figures indicate the scan number.)

Deaerated acetonitrile (10 mL) was then introduced into the cell to form $TBAPF_6$ solution. After circulation of the solution through the alumina-filled column, pyrrole and HCl (when needed) were added to the cell without contact with the alumina column. All steps of the cell-opening operation were protected by argon.

Voltammetric Measurement. A Pt disk (diameter 1 mm, area 0.785 mm^2) sealed in a soft glass rod was used as the working electrode; it was polished with diamond (0.25 mm) polishing paste and then rinsed thoroughly with ethanol and acetone. Pt and Ag wires were used as counter and quasireference electrodes, respectively. Potentials versus the Ag quasireference electrode were then rescaled by Ag/AgCl, which was calibrated with the ferrocene/ferrocenium redox couple (0.35 V vs Ag/AgCl). An EG&G potentiostat/galvanostat model 273 and a Kipp & Zonen Delft BV BD 92 recorder were used for electrochemical control and data recording. The scan rate in all experiments was 100 mV s^{-1}.

EQCM. AT-cut quartz crystals (5 MHz) of 15-mm diameter were obtained from Kristall-Verarbeitung Neckarbischofsheim GmbH. Both sides of the quartz crystals were coated with platinum by vacuum deposition. An underlayer of chromium was used to improve the mechanical stability of the platinum films. The oscillating area was 0.28 cm^2. The quartz was clamped between two O-rings. The details of the EQCM setup were described in ref 17. A Hameg HM 2122 frequency counter connected with an IEEE-488 interface bus to an IBM personal computer was used to measure the resonance frequency. The voltammetric experiments were performed using a three-electrode potentiostat (Amel model 533) connected via an A/D−D/A converter to the computer. Homemade software was used for data processing.

In Situ Conductivity. In situ conductivity measurements were carried out on a microarray working electrode (5 μm gap). The working electrode was separated from the potentiostat by two 1-kΩ resistors. A bias of $E = 10$ mV was applied to the microarray electrode and a third 1-kΩ resistor at which the potential was measured. The conductivities of the polymers on the microarray electrode were calculated according to the ohmic rules. This setup was controlled by an AMEL 553 potentiostat, and the potential scans were performed with an EG&G/PAR model 175 scan generator. Further details have been published previously.[9]

Results and Discussion

Galvanostatical Synthesis. In the first paper of this multipart account,[5] we showed the possibility of preparing PPy(II) in a solution of acetonitrile, which was used as received. Because of the uncertainty of the residual acid in acetonitrile and the high susceptibility of PPy(II) formation to acidity,[6] the preparation of PPy(II) in an untouched acetonitrile solution is difficult to reproduce, but in an acetonitrile solution containing 1×10^{-5} M HCl and 1 wt % H_2O, PPy(II) is readily and reproducibly formed from 0.1 M pyrrole when lower switching potentials are applied. However, a thick film of PPy(II) is difficult to achieve by potentiodynamic synthesis because of proton enrichment in the reaction zone as a result of a faster reaction rate at a later stage of film growth. Only at a very low, controlled current level can the condition of weak acidity, which is crucial to the formation of PPy(II), be maintained during the whole process of polymerization. Films prepared in this way are homogeneous throughout the thickness profile.

Figure 1 shows different CVs of PPy variants, galvanostatically prepared at different currents in identical solution, in a

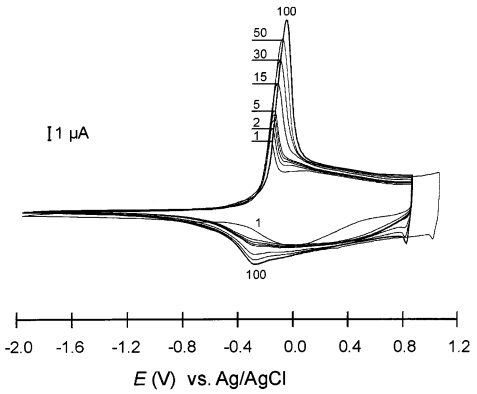

Figure 2. Redox behavior of galvanostatically prepared PPy(II) in monomer-free solution. Monomer-free solution: 0.1 M $TBAPF_6$ in acetonitrile, 100 mV s^{-1}, −20 °C. Preparation solution: 0.1 M pyrrole, 0.1 M $TBAPF_6$, 1 wt % H_2O, 1% 10^{-5} M HCl in acetonitrile, −20 °C. Current/charge: 50 nA/360 μC. (Figures indicate the scan number.)

monomer-free cell. The preparation current decreases from Figure 1A−H. Under high current density (25 mA/cm^2), the proton release from coupling reactions causes the reaction zone to become highly acidic, and acid-catalyzed trimerization of pyrrole occurs. The simultaneous oxidative polymerization of pyrrole trimer (i.e., 2,2′-(2,5-pyrrolidinediyl)dipyrrole[6−8]) and pyrrole results in the partially conjugated and cross-linked copolymer PPy(III),[6,8] which exhibits symmetrical anodic and cathodic waves (Figure 1A). Lowering the galvanostatic current increases the conjugation length of the resulting copolymer and produces a polymer that exhibits, to some degree, the features of PPy(I). This case is shown in Figure 1B. By lowering the current further, we observed the formation of PPy(I) over a wide current range. From Figure 1C−E, the current decreases by a factor of 50 (12.5 mA/cm^2 − 0.25 mA/cm^2), but no significant change in the CVs can be found.

When the current was decreased to 0.5 μA (60 μA/cm^2), the oxidation peak of PPy(II) began to appear. In monomer-free solution, after the polymer had undergone several potential cycles from 0.71 to −1.99 V (possibly the polymer was structurally relaxed during redox switching), the initial oxidation wave split into two peaks corresponding to the oxidation of PPy-(I) and PPy(II). Parallel to the change in the anodic curve, the cathodic curve displays a state between pure PPy(I) and pure PPy(II). Pure PPy(II) with an oxidation peak at −0.23 V can be synthesized at an even lower current (100 nA = 12 μA/cm^2 and 50 nA = 6 μA/cm^2 in Figure 1G and H, respectively).

As we pointed out before, the as-prepared PPy(II) exhibits two notable features. First, the reduction behavior in the first scan from the oxidized state to the neutral state is different from the behavior in subsequent scans. Second, the as-prepared polymer is not as highly charged as it could be, as the ever-increasing redox waves demonstrate (Figure 1G and H). In Figure 1H, the redox charge in one cycle becomes constant after many scans. The amount of the stable charging/discharging is approximately double that in the first scan. The charging difference between the stabilized state and the as-prepared state increases with the decrease of temperature at which the PPy-(II) is synthesized. Films prepared at −20 °C show a larger change in their charging/discharging capacity when the films undergo repetitive scans in monomer-free solution. This is obvious in Figure 2. Although the abnormal behavior that occurs during the first reduction scan of as-prepared PPy has been discussed by several authors,[4b,10] the unsaturated charging state displayed by as-prepared PPy(II) was first reported by us.[5]

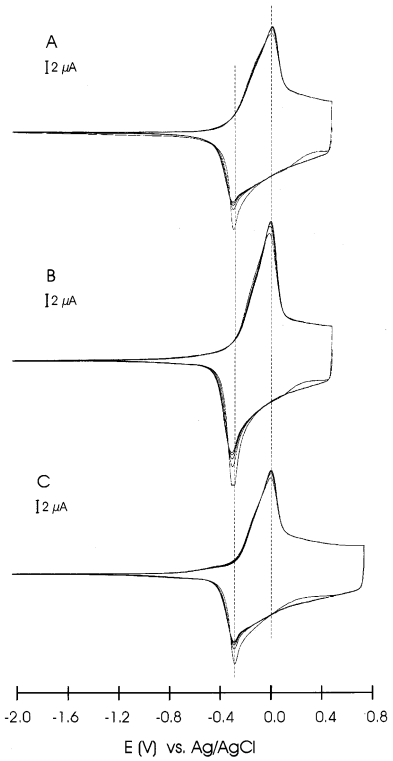

Figure 3. CVs of PPy(I) galvanostatically prepared in solventless pyrrole solution. Monomer-free solution: 0.1 M $TBAPF_6$ in acetonitrile, 100 mV s^{-1}, 0 °C. Preparation solution: 0.1 M $TBAPF_6$, 1 wt % H_2O in pyrrole, 0 °C. (A) 50 nA/600 μC, 0.46 to −2.04 V; (B) 0.5 μA/600 μC, 0.46 to −2.04 V; (C) 5 μA/602.8 μC, 0.71 to −2.04 V.

During the potential scan in monomer-free solution, applying higher potential leads the PPy(II) to approach its final stable state more quickly.

Among the PPy variants, PPy(I) and PPy(II) are better defined than PPy(III). Experimental conditions tend to favor the formation of PPy(I); therefore, in most cases, the resulting polymer is a PPy(I)-predominated material with minor portions of PPy(II) or PPy(III). Well-formed PPy(I) has a well-shaped CV such as Figure 1D.

The conditions for the formation of PPy(II) are more subtle. In our previous discussion,[5,6] the applied potential and reaction rate were taken into consideration. However, in a acid-free solution treated with basic alumina, hardly any PPy(II) can be formed, even at an extremely low reaction rate, by applying an extremely low switching potential in potentiodynamical synthesis. Increasing the monomer concentration in the solution makes it possible to perform electropolymerization at an even lower potential or current. An extreme case is the electropolymerization of pyrrole in 0.1 M $TBAPF_6$/pyrrole solventless solution (contains no acetonitrile, but 1 wt % of water was added to the solution to prevent the protonation of pyrrole molecules during electropolymerization). In this case, sustainable electrooxidation and electropolymerization of pyrrole can proceed at a potential of less than 0.45 V. However, no strong features of PPy(II) can be found voltammetrically. In Figure 3, we see almost the same CVs of PPy(I) from three films galvanostatically prepared at currents of 50 nA ↔ 6 μA/cm^2 (corresponding potential ca. 0.46 V), 0.5 μA, and 5 μA ↔ 0.6 mA/cm^2 (corresponding potential ca. 0.71 V). A small shoulder at a potential of −0.23 V indicates that the formation of PPy(II) does not exceed 20%. Together with previous observations, this result rules out the possibility that a slow reaction or a low potential alone causes the formation of PPy(II).

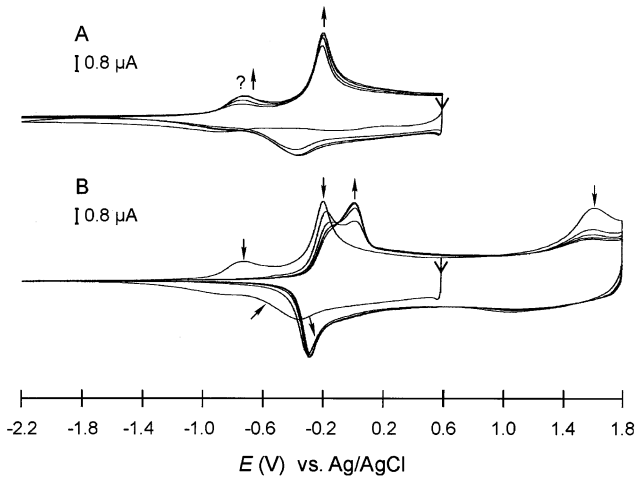

Figure 4. Electrochemical solid-state transition of PPy(II) to PPy(I). Monomer-free solution: 0.1 M $TBAPF_6$ in acetonitrile, 100 mV s^{-1}, −20 °C. Preparation solution: 0.1 M pyrrole, 0.1 M $TBAPF_6$, 1 wt % H_2O, 1% 10^{-5} M HCl in acetonitrile, 20 °C. Current/charge: 100 nA/150 μC. (A) 0.60 to −2.2 V; scans 1, 2, 5, and 10; (B) after 12 scans in the range of 0.60 to −2.2 V, the scan range was extended to 1.8 to −2.2 V.

All of the results obtained up to now indicate that the proton concentration is an additional factor among the experimental variables. In our electrolytic system, when the proton concentration is kept at 1×10^{-5} M and current density is kept below about 25 μA/cm^2, PPy(II), showing an oxidation peak at −0.23 V, can be readily and reproducibly prepared.

Electrochemical Solid-State Transition from PPy(II) to PPy(I). As mentioned above, a higher potential facilitates the charging saturation of PPy(II) during repetitive potential scans in monomer-free solution. However, when the potential exceeds a certain value, a drastic change in polymer structure occurs (i.e., a solid-state transition from PPy(II) to PPy(I)).

Figure 4 shows the transition clearly when a switching potential of 1.8 V was applied. The redox states of the galvanostatically prepared PPy(II) film were initially switched in the potential range of 0.60 to −2.2 V. After 12 scans, during which the potential scan range was extended to 1.8 to −2.2 V, an irreversible anodic wave appears at about 1.6 V. The immediate discharging scan generated a sharper, positively shifted reduction wave. By continuous scanning in the range of 1.8 to −2.2 V, the oxidation peak at −0.23 V gradually disappeared while a peak emerged at ca. 0.0 V. The final CV is identical to that of PPy(I). This is a clear indication of the transition from PPy(II) to PPy(I) after the irreversible solid-state oxidation at ca. 1.6 V.

The positive switching potential in Figure 4B was set higher than the peak potential of the irreversible oxidation process. If the positive switching potential is set in the ascent of the irreversible wave, the transition also takes place, though at a lower rate. In Figure 5, starting from the first reduction scan of an as-prepared PPy(II) film, a series of potential scans are carried out that reveal comprehensively the voltammetric properties of PPy(II). Figure 5A shows that the as-prepared PPy(II) becomes fully charged in 35 scans. Further scans between 0.27 and −2.03 V indicate high stability of the fully charged PPy(II) (Figure 5B). However, when the positive switching potential is set at 1.57 V, at which the irreversible oxidation occurs, PPy(II) begins to transform into PPy(I). Gradually enhancing the switching potential brought the transition to completion. After 10 scans (Figure 5C), the 61st cycle gives an almost perfect CV of PPy-(I) (compare Figure 5D). Now, as indicated by Figure 5D,

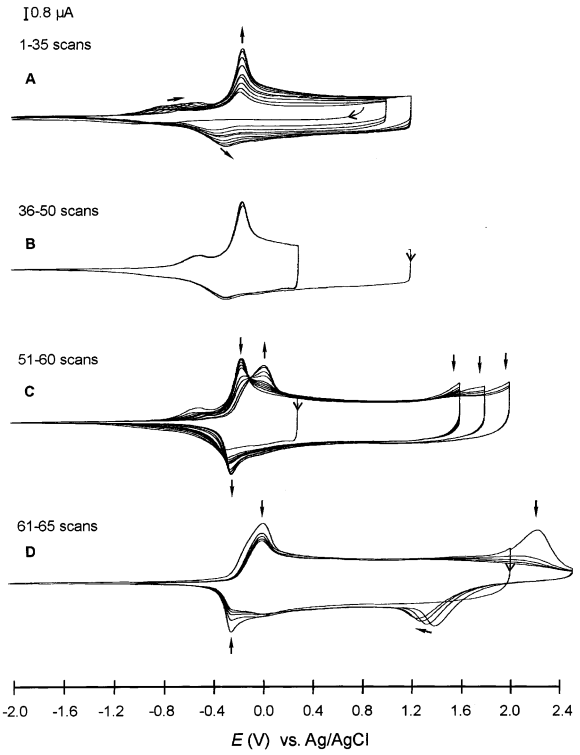

Figure 5. Continuous change of CVs upon extension of potential scan range. Monomer-free solution: 0.1 M $TBAPF_6$ in acetonitrile, 100 mV s^{-1}, −20 °C. Preparation solution: 0.1 M pyrrole, 0.1 M $TBAPF_6$, 1 wt % H_2O, 1% 10^{-5} M HCl in acetonitrile, 20 °C. Current/charge: 200 nA/165 μC. (A) Scans 1−35 and 1−7, 0.79 to −2.03 V (scans 1, 2, 4, and 7) then 0.97 to −2.03 V (scans 8, 12, 17, 25, and 35; (B) scans 36−50, 0.27 to −2.03 V (scans 36, 37, and 50); (C) scans 51−60, 1.57 to −2.03 V, 1.77 to −2.03 V, 1.97 to −2.03 V; (D) scans 61−65, 1.97 to −2.03 V, 2.47 to −2.03 V.

applying an even higher potential (>2.0 V) to PPy(I) irreversibly oxidizes PPy(I) and makes it electrochemically inactive.

Mechanistic Pathways of the Formation of PPy(II) and PPy(I). The electrochemical solid-state transition from PPy(II) to PPy(I) raises a question about the structure of the both PPy variants and the transition process. Solid-state polymerization of oligomers of *p*-phenylene and α-thiophene has been described by Meerholz and Heinze.[11] Because the phenomenon illustrated in Figures 4 and 5 is quite similar to solid-state polymerization, the transition from PPy(II) to PPy(I) may also imply the oxidative coupling of shorter chains of PPy(II) to longer chains of PPy(I). To support this assumption, two obstacles must be overcome.

First, as thoroughly discussed previously,[5,6] the oxidation potentials of PPy(I) and PPy(II) do not match the chain-length/potential relation.[11c, 12] Second, the extrapolation of the oxidation potentials of pyrrole oligomers shows that the oxidation potential of PPy(II) is more negative than the extrapolated value[13,14] for the "infinite" polymer.

A plausible explanation was proposed to overcome the first obstacle:[15] in terms of chain length, PPy(II) may have shorter chains, whereas PPy(I) could be considered to be a polymer with physically longer chains. However, a physically longer chain does not necessarily mean a longer conjugation. Because of the increased possibility of cross linking (i.e., network formation) and other chain defects, a longer chain may have a shorter conjugation length. However, PPy(II), though physically shorter, may have a longer conjugation. Hence, the oxidation potential of PPy(II) is more negative than that of PPy(I). We now believe that this interpretation is incorrect.

SCHEME 1: Reaction Scheme of Pyrrole in Dry Acetonitrile

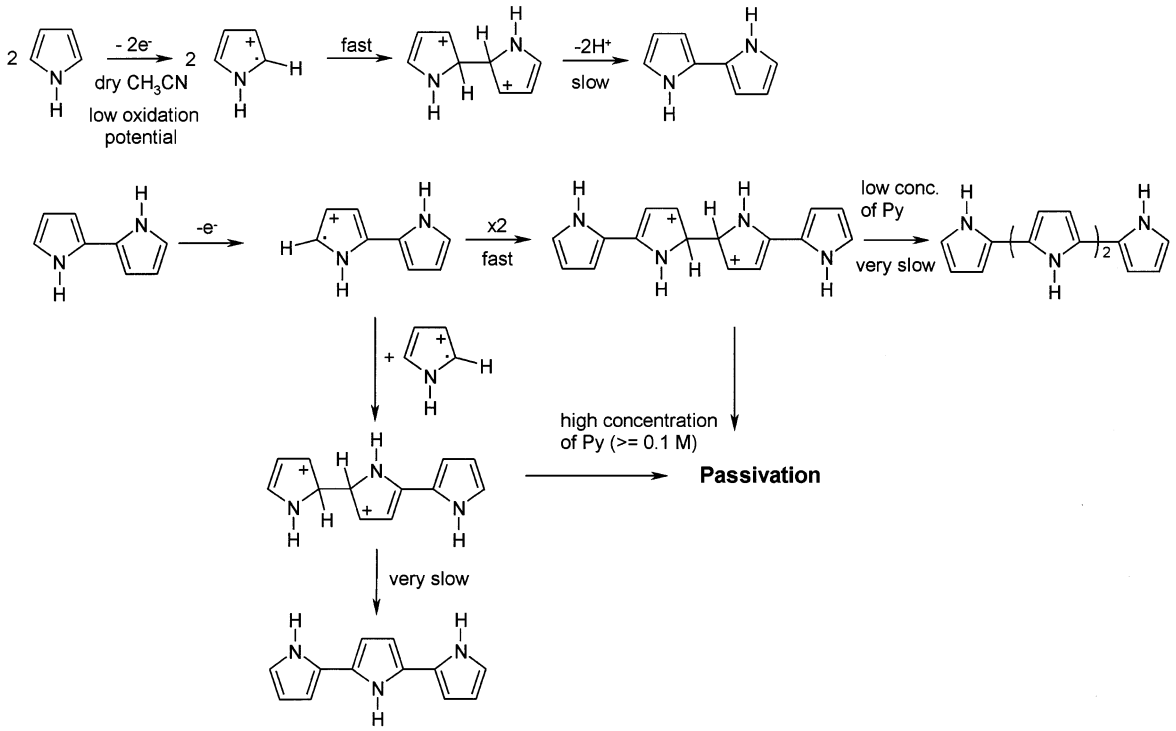

A second explanation is based on the assumption that in the solid state the charging steps of chainlike conjugated oligomers and polymers are correlated with an overpotential that may be caused by the additional energy needed to flatten tilted chains. Because chain length and the tendency for network formation with significant distortions are greater in PPy(I) than in PPy(II), the overpotential of the latter should be lower. In our opinion, experimental data clearly support the view that the strong positive shift of the oxidation waves is due to overpotential effects caused by tilted chains. Recent experiments carried out at very low scan rates (0.01 mV/s) reveal that the oxidation of PPy(I) starts at potentials that are significantly lower than those observed at normal scan rates (∼100 mV/s). This gives clear evidence for the postulated overvoltage effect.

This raises further questions concerning the effect of protons. Why, at the same low potential or reaction rate, does PPy(I) form better in the absence of protons but pure PPy(II) is formed only at proton concentrations of about 10^{-5} M?

The second inconsistency, namely, the low oxidation potential of PPy(II) in comparison to that of the infinite polymer, may result from the small number of experimental data available for monodisperse pyrrole oligomers. In particular, no precise thermodynamic redox potentials have been measured for longer oligomers (≥ 7) in these series.

Recently, we have studied the coupling steps of well-defined methoxy-substituted oligothiophenes after their anodic oxidation. Interestingly, all results clearly show that the rate constant of the second-order coupling steps between chainlike oligomers gradually decreases as a function of chain length.[16] However—and this is even more noteworthy—the rates of proton elimination from the "dimeric" coupling intermediates diminish so drastically that charged σ dimers with more than four units in one conjugated chain segment are fairly stable in the charged state. Proton elimination from such species takes place only when the σ intermediates are oxidized to a higher charging level, which increases the reactivity of the system. Hapiot reported that radical cations of oligopyrroles and their coupling intermediates are stabilized with increasing chain length.[17] The reason for this effect is that the acidity of proton-containing coupled σ intermediates decreases as a function of chain length. The stabilization of the positive charges depends on electronic factors and the extent of the conjugated system. Thus, σ dimers of the pyrrole series are more stable than the corresponding thiophene oligomers, and the chain-length criterion provides greater stability—meaning a lower tendency for proton release—of such intermediates with increasing chain length. An important consequence of this behavior is that oligomeric chains cannot grow via the coupling of a monomeric species with an oligomeric chain because the resulting intermediates do not eliminate protons. As has been shown, the formation of conducting polymers proceeds within a cascade of dimerization steps, leading to oligomeric species in solution and, after deposition, to a polymeric system in the solid state.[9] An essential prerequisite for successful polymerization is a sufficiently "strong" base in the solution to accept protons from the σ intermediates. In the case of protonated pyrroles, the pK_a value lies between 4 and −4, whereas the pK_a value of acetonitrile is approximately −10. Therefore, the oligomerization of pyrrole in pure acetonitrile may have already stopped at the level of the σ intermediate of bipyrrole, or side reactions that are dominant at high pyrrole concentrations may cause the formation of a passivating layer[6b] (Scheme 1). Acetonitrile is a weaker base than the σ intermediate. Consequently, a stronger base must be used to initiate the elimination of protons. Water fulfills this condition. A similar effect results from the application of a sterically hindered base such as 2,6-di-*tert*-butylpyridine.[18] However, the concentration should be kept low because at high concentrations proton abstraction from the monomeric radical cation may occur. Our experimental data reveal that at a pyrrole concentration from 10^{-3} to 10^{-2} M the same amount of pyridine base is sufficient for a high yield of PPy(I).[3b,19] Normally, in acetonitrile in the presence of 1% of water, PPy(I) is generated.

The galvanostatic conditions for the generation of PPy(II) correspond to an oxidation potential of 0.46 V versus Ag/AgCl,

SCHEME 2: Possible Reaction Path for the Polymerization of Pyrrole

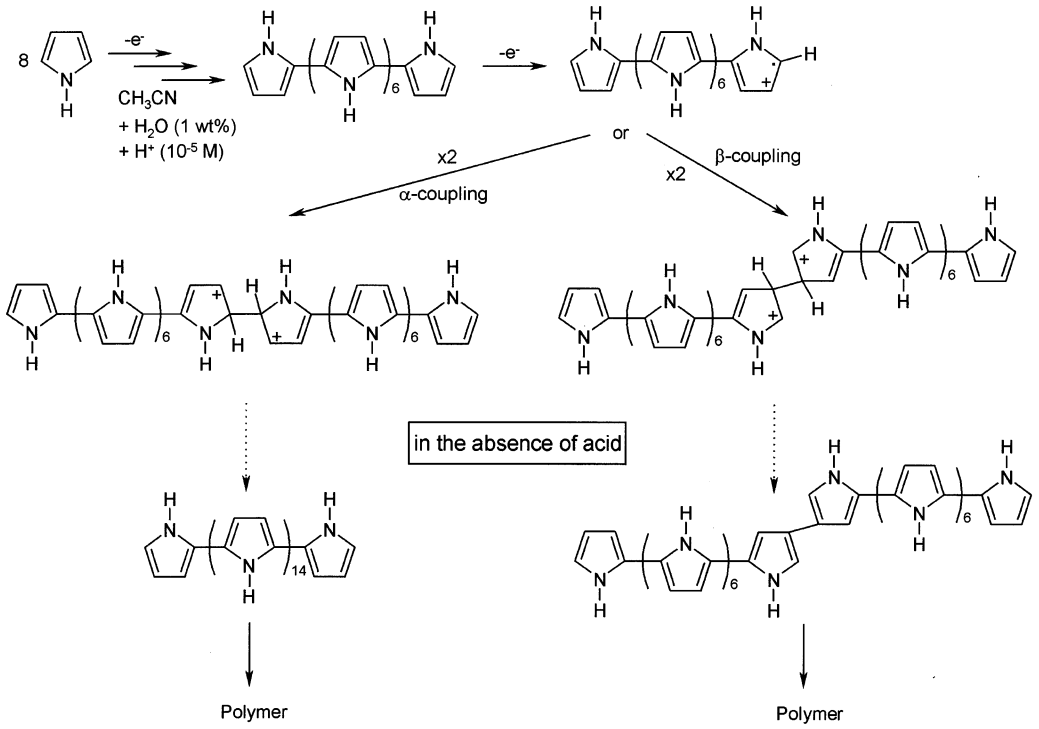

which is higher than that of quaterpyrrole but still below the redox potential of dication formation. Thus, it is reasonable to assume that quaterpyrrole, which is formed in solution in two successive coupling steps, is oxidized and slowly eliminates protons after its dimerization. The octapyrrole formed is deposited on the electrode.[12,20] Because of the electrochemical conditions, the octamer is charged and couples, despite a low second-order rate constant (the surface concentration of the octamer is high), to form a σ dimer containing 16 pyrrole units (Scheme 2). The fact that protons are available at a concentration of 1×10^{-5} M prevents the deprotonation of this σ dimer but does not initiate acid-catalyzed trimerization and polymerization reactions to form pyrrolidine units. The stabilizing effect of a small amount of acid was also observed in the case of the oligomerization of quaterthiophene, where the addition of a small amount of acid stopped the polymerization process.[21] Obviously, both the applied oxidation potential and the proton concentration in front of the electrode steer the oligomerization and polymerization steps of pyrrole. Therefore, we assume that oxidized octameric chains undergo slow intermolecular coupling reactions via α,α' or β,β' bond formation between two pyrrole units, forming two sp^3 centers with localized charges in these moieties. In the presence of a small amount of acid, the reaction stops at this level because of the low acidity of the dimeric system (Scheme 2). However, in a pure pyrrole solution, pyrrole acts as a base, and protons are released from the charged σ dimer, producing a neutral species that can be oxidized again and then undergo the next coupling reaction, leading to the formation of PPy(I). Similarly, in the presence of water without any addition of acid, the tendency is to form PPy(I).

Because the positive charges in the coupled pyrrole units, which still contain protons at the coupling sites, are immobile, the discharging of such a system cannot occur by a simple hopping of the positive charges to the metallic electrode surface and a simultaneous ejection of anions into the solution. To maintain the condition of electroneutrality, positively charged co-ions must be incorporated into the polymeric layer during the discharging reaction. This process is slow and strongly temperature-dependent. Thus, quite a large number of potentiodynamic cycles are necessary to discharge the system completely and open channels for inserting large co-ions such as tetrabutylammonium cations. Consequently, the film can be fully charged only after this "activation" of the layer has been completed.

EQCM Study. Ion movement during redox switching of PPy has been extensively studied in the past using the EQCM technique. Early work confirmed the accompanying insertion and expulsion of anions during the redox transition of the polymer.[22] Smyrl et al.[23] reported that ionic movement depends greatly on the size of the anion. PPy films doped exclusively with small anions such as ClO_4^- and BF_4^- showed anion transport during redox transition. For the PPy films doped with large polymeric anions such as poly(4-styrenesulfonate) and polyvinylsulfonate, for the most part, cations and solvent molecules were inserted and removed to compensate for the charge on PPy. The films formed with medium-sized anions (tosylate) showed both apparent anion and cation motion during the redox process. Heinze and Bilger[24] found that in the $LiClO_4$−propylene carbonate solution the relative contributions of anions and cations depend strongly on the potentials at which the PPy films are formed. During the redox process, a PPy film prepared at a potential of 1.0 V shows a uniform mass change, which can be interpreted to result from anion transport, whereas a PPy film formed at a potential of 0.7 V exhibits two-stage mass changes, which can be explained by the movement of both anions and cations. Kontturi et al.[25] obtained similar results from aqueous sodium tosylate solutions.

Having recognized the voltammetric differences between PPy variants prepared at different potentials, we can provide more knowledge of the mass change during the redox process. Figure 6 depicts both current change and mass change (represented by the frequency change in a quartz crystal). In Figure 6A, one can see that the redox process of PPy(II) is accompanied by the movement of both anions and cations. That is, during reduction, the film first becomes light (because of the release of anions) and then heavy (because of the insertion of cations),

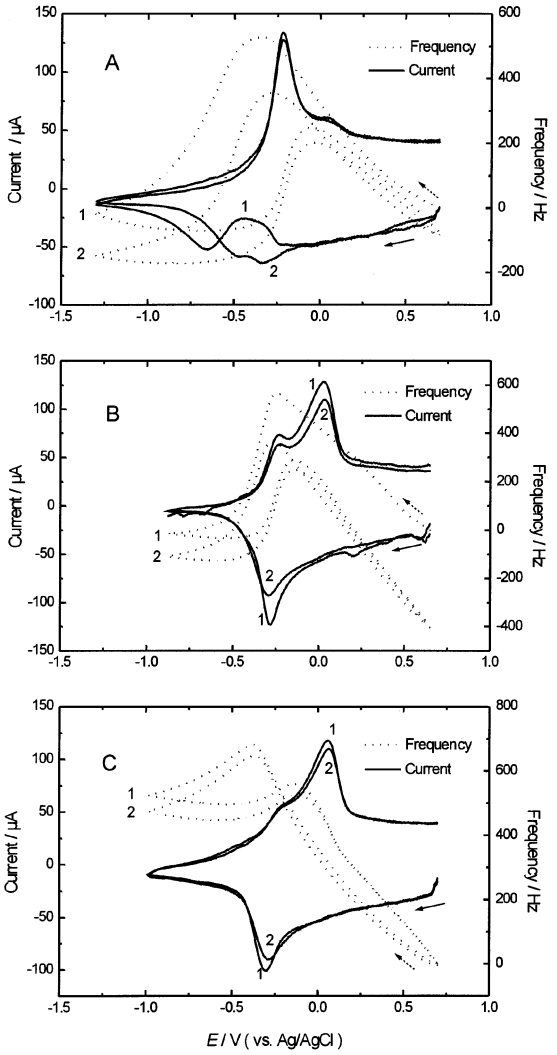

Figure 6. EQCM studies on PPy films formed galvanostatically at different currents. Monomer-free solution: 0.1 M $TBAPF_6$ in acetonitrile, 20 mV s^{-1}, 20 °C. Preparation solution: 0.1 M pyrrole, 0.1 M $TBAPF_6$, 1 wt % H_2O, 1% 10^{-5} M HCl in acetonitrile, 20 °C. (A) 15 μA (55 μA/cm^2); (B) 30 μA (110 μA/cm^2); (C) 60 μA (220 A/cm^2).

whereas during reoxidation, the film first releases the cations and then incorporates the anions. The mass change induced by anion transport is almost the same as that induced by cation transport. Therefore, in a half-cycle (reduction or oxidation), the net mass change is approximately zero. For a polymer composed of both PPy(II) and PPy(I), the contribution of the cation to the mass change is less than that of the anion (Figure 6B). Further increases of the PPy(I) component in the polymer results in the anion movement dominating the cation movement (Figure 6C). If the PPy(I) film is prepared in a form free of PPy(II), the insertion/repulsion of cation can never be observed. During the redox process, the mass changes uniformly (i.e., monotonically decreases upon reduction and increases upon oxidation).

The data shown in Figure 6 clearly indicate that single-anion transport is a feature of PPy(I) during the redox process, whereas PPy(II) exhibits the movement of both anions and cations. Because PPy(II) is formed at lower potentials or current levels, these results are consistent with those reported by other authors.[24,25] As was discussed in a previous report,[5] in $LiClO_4$−acetonitrile solution, the separation of peak potentials between PPy(I) and PPy(II) is very small, and the difference between PPy(I) and PPy(II) is not voltammetrically apparent. Neverthe-

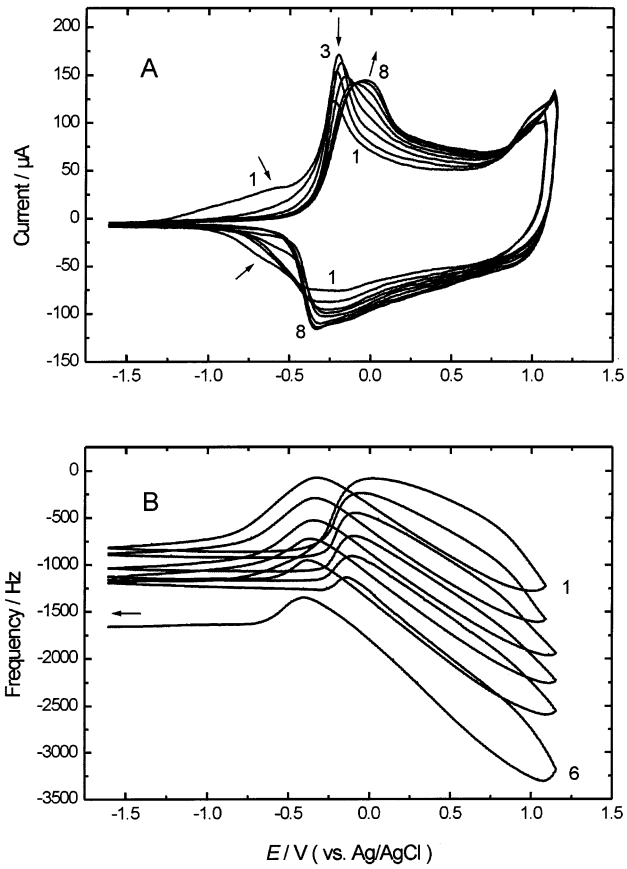

Figure 7. EQCM studies on the transition from PPy(II) to PPy(I). Monomer-free solution: 0.1 M $TBAPF_6$ in acetonitrile, 20 mV s^{-1}, 20 °C. Preparation solution: 0.1 M pyrrole, 0.1 M $TBAPF_6$, 1 wt % H_2O, 1% 10^{-5} M HCl in acetonitrile, 20 °C, 15 μA (55 μA/cm^2)/5000 Hz. (A) Voltammetric change upon solid-state transition; (B) mass change.

less, the behavior of mass change during redox switching can clearly differentiate the natures of the polymer films.[24]

The results of the EQCM experiments show that the discharging of PPy(II) mainly involves the insertion of cations. This surprising observation can be easily explained on the basis of the "high density" of σ-coupled pyrrole units. The latter one form sp^3 centers with localized positive charges. Consequently, anions in the film do not move, and cations are incorporated during discharging to maintain electroneutrality. This effect is predominant in a film that contains small amounts of solvent and electrolytes but weakens after several charging−discharging cycles during which solvent and electrolytes are inserted into the film and enlarge the polarity of the material.

The different nature of mass change in PPy(I) and PPy(II) was also consistently demonstrated in Figure 7, which shows the changes of the voltammogram and the mass during the transition from PPy(II) to PPy(I). At the beginning, the as-prepared PPy(II) film exhibited nearly equal contributions of anions and cations to the mass change (see the first cycle in Figure 7B). During the transition process, the contribution of cations gradually decreased. After six cycles, the transition of PPy(II) to PPy(I) is nearly complete, and charge compensation during the redox process is achieved by anion movement.

In Situ Conductivity Measurement. The in situ conductivity measurements carried out during voltammetric charging and discharging of PPy(I), PPy(II), and PPy(III) reveal that all structures of polypyrrole become conductive during the oxidation of the polymer. Nevertheless, the increase in conductivity as a function of doping is different for all three polypyrroles.

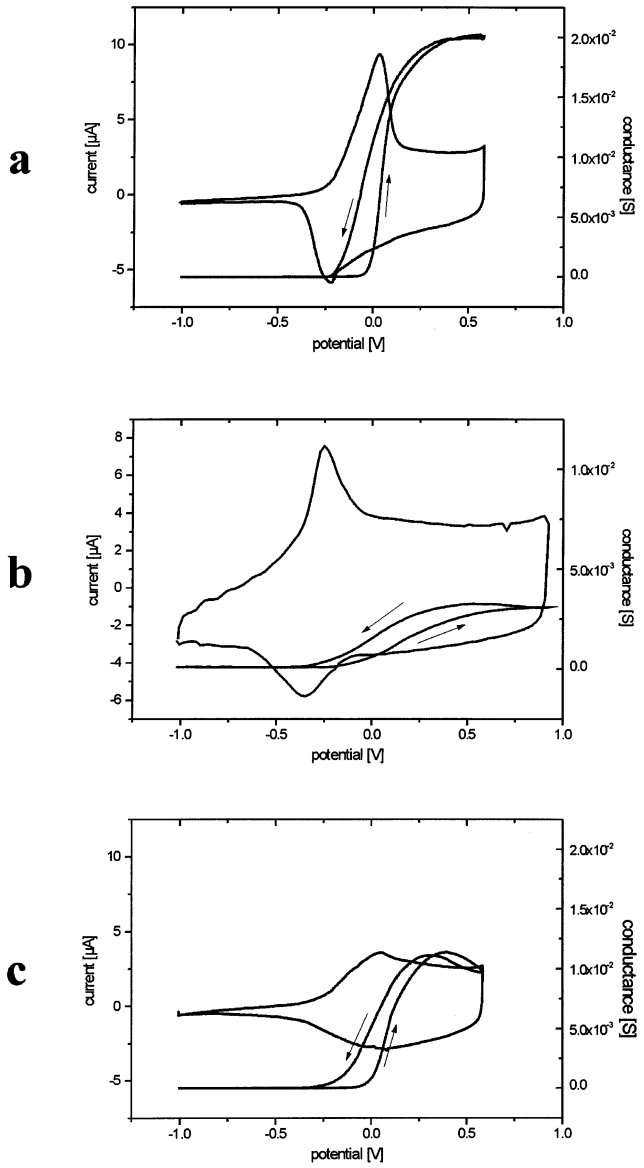

Figure 8. In situ conductivity measurements of (a) PPy(I), (b) PPy-(II), and (c) PPy(III). Monomer-free solution: 0.1 M $TBAPF_6$ in acetonitrile, 5 mV s^{-1}, 20 °C.

In the case of PPy(II), the highest conductivity is observed after passing the main oxidation wave of the electroactive material, whereas for PPy(I) and PPy(III), the conductivity reaches its maximum within the first oxidation wave.

During discharging, a pronounced hysteresis of the conductivity can be observed. The hysteresis indicates that during charging some structural changes occur, which may include flattening of twisted chains and the formation of σ bonds between pyrrole moieties of different chains. Both effects stabilize the charged state but have different influences on the conductivity. Thus, flattening improves the conjugation and therefore facilitates charge transport through hopping. However, the σ dimerization creates sp^3 centers in the pyrrole rings and as a consequence produces immobile charge carriers. After discharging, the system slowly relaxes and returns to its initial state. We believe that the memory effect is also based on this slow relaxation process. Recent measurements provide evidence that the decay of the σ dimers in the polymeric layer has a small rate constant.[9b]

In the case of PPy(II), where the portion of σ dimers is substantial, a high charging level is necessary in order to approach a conductivity on the order of 1−10 S/cm. For PPy-(I), and in particular for PPy(III), the portion of σ dimers is lower. Therefore, there is appreciable conductivity at a relatively low level of charging.

Conclusions

We are now able to prepare specifically the previously described PPy variants under well-defined conditions. Galvanostatical polymerization of the different types of PPy is a function of current density and proton concentration and is therefore independent of film thickness. In our work, the solid-state transition from PPy(II) to PPy(I) was consistently investigated and related to chain length and network formation for the first time.

EQCM and conductivity measurements clearly indicate that there are structurally different types of PPy. PPy(I) and PPy-(III) show only anion movement, whereas PPy(II) shows movement of both anions and cations. There are two types of charge carriers in the different PPy variants: mobile carriers, which contribute to overall conductivity, and immobile carriers, which do not contribute to conductivity but give rise to cross-linking involving network formation and therefore structural diversity. Structural information should be a subject of future research.

Acknowledgment. Dr. Ming Zhou is grateful to the Alexander von Humboldt Foundation for an Alexander von Humboldt Research Fellowship. Financial support of the DFG and Fonds der Chemischen Industrie is gratefully acknowledged.

References and Notes

(1) (a) Diaz, A. F.; Kanazawa, K. K.; Gardini, G. P. *J. Chem. Soc., Chem. Commun.* **1979**, 635−636. (b) Kanazawa, K. K.; Diaz, A. F.; Geiss, R. H.; Gill, W. D.; Kwak, J. F.; Logan, J. A.; Rabolt, J. F.; Street, G. B. *J. Chem. Soc., Chem. Commun.* **1979**, 854−855. (c) Kanazawa, K. K.; Diaz, A. F.; Gill, W. D.; Grant, P. M.; Street, G. B.; Gardini, G. P.; Kwak, J. F. *Synth. Met.* **1979**−**1980**, *1*, 329−336. (d) Diaz, A. F.; Castillo, J. L.; Logan, J. A.; Lee, W. Y. *J. Electroanal. Chem.* **1982**, 118−129.

(2) Tourillon, G.; Garnier, F. *J. Electroanal. Chem.* **1982**, *135*, 173−178.

(3) (a) Andrieux, C. P.; Audebert, P.; Hapiot, P.; Savéant, J.-M. *J. Am. Chem. Soc.* **1990**, *112*, 2439−2440. (b) Andrieux, C. P.; Audebert, P.; Hapiot, P.; Savéant, J.-M. *J. Phys. Chem.* **1991**, *95*, 10158−10164.

(4) (a) *Handbook of Conducting Polymers;* Skotheim, T. A., Ed.; Marcel Dekker: New York, 1986. (b) Heinze, J. *Top. Curr. Chem.* **1990**, *152*, 1−47. (c) Roncali, J. *Chem. Rev.* **1992**, *92*, 711−738.

(5) Zhou, M.; Heinze, J. *Electrochim. Acta* **1999**, *44*, 1733−1748.

(6) (a) Zhou, M.; Heinze, J. *J. Phys. Chem. B* **1999**, *103*, 8443. (b) Zhou, M.; Heinze, J. *J. Phys. Chem. B* **1999**, *103*, 8451.

(7) (a) Potts, H. A.; Smith, G. F. *J. Chem. Soc.* **1957**, 4018−4022. (b) Smith, G. F. *Adv. Heterocycl. Chem.* **1963**, *2*, 287−309. (c) Otero, T. F.; Rodríguez, J. *J. Electroanal. Chem.* **1994**, *379*, 513−516. (d) Lamb, B. S.; Kovacic, P. *J. Polym. Sci., Polym. Chem. Ed.* **1980**, *18*, 1759−1770.

(8) Zhou, M.; Rang, V.; Heinze, J. *Acta Chem. Scand.* **1999**, *53*, 1059.

(9) (a) Smie, A.; Synowczyk, A.; Heinze, J.; Alle, R.; Tschuncky, P.; Götz, P.; Bäuerle, P. *J. Electroanal. Chem.* **1998**, *452*, 87−95. (b) Pagels, M.; Heinze, J.; Geschke, B.; Rang, V. *Electrochim. Acta* **2001**, *46*, 3943−3954.

(10) (a) Heinze, J.; Störzbach, M.; Mortensen, J. *Ber. Bunsen-Ges. Phys. Chem.* **1987**, *91*, 960−967. (b) Li, Y. *Electrochim. Acta* **1997**, *42*, 203-210.

(11) (a) Meerholz, K.; Heinze, J. *Angew. Chem., Int. Ed. Engl.* **1990**, *29*, 692−694. (b) Meerholz, K.; Heinze, J. *Angew. Chem.* **1990**, *102*, 655−697. (c) Meerholz, K.; Heinze, J. *Electrochim. Acta* **1996**, *41*, 1839−1854.

(12) Heinze, J.; Tschuncky, P. *Electronic Materials: The Oligomer Approach;* Müllen K., Wegner, G., Eds.; Wiley-VCH: 1998; pp 479−514.

(13) Zotti, G.; Martina, S.; Wegner, G.; Schlüter, A. D. *Adv. Mater.* **1992**, *4*, 798−810.

(14) Andrieux, C. P.; Hapiot, P.; Audebert, P.; Guyard, L.; Nguyen Dinh An, M.; Groenendaal, L.; Meijer, E. W. *Chem. Mater.* **1997**, *9*, 723−729.

(15) Proposed by one of the referees of ref 5.

(16) Heinze, J.; John, H.; Dietrich, M.; Tschuncky, P. *Synth. Met.* **2001**, *119*, 49−52.
(17) (a) Andrieux, C. P.; Hapiot, P.; Audebert, P.; Guyard, L.; Nguyon Dinh An, M.; Groenendaal, L.; Meijer, E. W. *Chem. Mater.* **1997**, *9*, 723. (b) Guyard, L.; Hapiot, P.; Neta, P. *J. Phys. Chem. B* **1997**, *101*, 5698.
(18) (a) Heinze, J.; Hinkelmann, K.; Land, M. *DECHEMA Monogr.* **1988**, *102*, 75−87. (b) Hammerich, O.; Henriksen, R. M.; Kumounah, F. S.; Hansen, G. H.; Lund, T. Abstract 1169, 2001 ECS Meeting, San Francisco, Sept 2−7, 2001.
(19) (a) Quian, R.; Pei, Q.; Huang, Z. *Makromol. Chem.* **1991**, *192*, 1263. (b) Visy, C.; Lukkari, J.; Kankare, J. *Synth. Met.* **1994**, *66*, 61−65.
(20) Heinze, J. In *Organic Electrochemistry*; Lund, H., Hammerich, O., Eds.; Marcel Dekker: New York, 2000; p 1309.
(21) Pagels, M.; Heinze, J., to be submitted for publication.
(22) Kaufman, J. H.; Kanazawa, K.; Street, G. B. *Phys. Rev. Lett.* **1984**, *53*, 2461.
(23) Naoi, K.; Lien, M.; Smyrl, W. H. *J. Electrochem. Soc.* **1991**, *138*, 440−445.
(24) Heinze, J.; Bilger, R. *Ber. Bunsen-Ges. Phys. Chem.* **1993**, *97*, 502−506.
(25) Kontturi, K.; Murtomäki, L.; Pentti, P.; Sundholm, G. *Synth. Met.* **1998**, *92*, 179−185.